The conserved *cis*-Pro[39] residue plays a crucial role in the proper positioning of the catalytic base Asp[38] in ketosteroid isomerase from *Comamonas testosteroni*

Gyu Hyun NAM*†, Sun-Shin CHA‡, Young Sung YUN*†, Yun Hee OH*†, Bee Hak HONG*†, Heung-Soo LEE‡ and Kwan Yong CHOI*†[1]

*National Research Laboratory of Protein Folding and Engineering, Pohang 790-784, Republic of Korea, †Division of Molecular and Life Sciences, Pohang University of Science and Technology, Pohang 790-784, Republic of Korea, and ‡Beamline Research Division, Pohang Accelerator Laboratory, Pohang 790-784, Republic of Korea

KSI (ketosteroid isomerase) from *Comamonas testosteroni* is a homodimeric enzyme that catalyses the allylic isomerization of Δ^5-3-ketosteroids to their conjugated Δ^4-isomers at a reaction rate equivalent to the diffusion-controlled limit. Based on the structural analysis of KSI at a high resolution, the conserved *cis*-Pro[39] residue was proposed to be involved in the proper positioning of Asp[38], a critical catalytic residue, since the residue was found not only to be structurally associated with Asp[38], but also to confer a structural rigidity on the local active-site geometry consisting of Asp[38], Pro[39], Val[40], Gly[41] and Ser[42] at the flexible loop between β-strands B1 and B2. In order to investigate the structural role of the conserved *cis*-Pro[39] residue near the active site of KSI, Pro[39] was replaced with alanine or glycine. The free energy of activation for the P39A and P39G mutants increased by 10.5 and 16.7 kJ/mol (2.5 and 4.0 kcal/mol) respectively, while ΔG_U^{H2O} (the free-energy change for unfolding in the absence of urea at 25.00 $\pm$ 0.02 °C) decreased by 31.0 and 35.6 kJ/mol (7.4 and 8.5 kcal/mol) respectively, compared with the wild-type enzyme. The crystal structure of the P39A mutant in complex with *d*-equilenin [*d*-1,3,5(10),6,8-estrapentaen-3-ol-17-one], a reaction intermediate analogue, determined at 2.3 Å (0.23 nm) resolution revealed that the P39A mutation significantly disrupted the proper orientations of both *d*-equilenin and Asp[38], as well as the local active-site geometry near Asp[38], which resulted in substantial decreases in the activity and stability of KSI. Upon binding 1-anilinonaphthalene-8-sulphonic acid, the fluorescence intensities of the P39A and P39G mutants were increased drastically, with maximum wavelengths blue-shifted upon binding, indicating that the mutations might alter the hydrophobic active site of KSI. Taken together, our results demonstrate that the conserved *cis*-Pro[39] residue plays a crucial role in the proper positioning of the critical catalytic base Asp[38] and in the structural integrity of the active site in KSI.

Key words: active-site geometry, *cis*-proline, ketosteroid isomerase, site-directed mutagenesis, structural integrity.

INTRODUCTION

The enzyme KSI (Δ^5-3-ketosteroid isomerase; EC 5.3.3.1) catalyses the allylic rearrangement of a variety of Δ^5-3-ketosteroids to Δ^4-3-ketosteroids by shifting a double bond from the 5(6)-position to the 4(5)-position (Scheme 1) [1]. KSI is one of the most efficient enzymes known, exhibiting a reaction rate equivalent to the diffusion-controlled limit [2]. It has been intensively investigated as a prototype to understand the catalytic mechanism of allylic rearrangement [3–7]. Structural analyses of two related KSI enzymes from different bacterial species, *Pseudomonas putida* biotype B and *Comamonas testosteroni*, by X-ray crystallography [8–10] and NMR spectroscopy [11,12] have contributed significantly to the understanding of the mechanism of efficient catalysis by KSI.

Although the KSIs from *P. putida* and *C. testosteroni* have only 34 % identity in their amino acid sequences, their three-dimensional structures are remarkably similar [8,9,11]. Moreover, three catalytic residues, Tyr[14], Asp[38] and Asp[99], play crucial roles in catalysis. The proton at C-4 of the steroid substrate is transferred to the catalytic base Asp[38] of the enzyme to generate the dienolate intermediate, which is stabilized by the hydrogen bonds of both Tyr[14] and Asp[99], and then the same proton is transferred to C-6 to generate the product (Scheme 1) [13–15]. Three catalytic residues are conserved in the two related KSIs (the residues are numbered according to those of *C. testosteroni* KSI throughout the text) [16–18]. Most notably, Asp[38] at the active site serves as a catalytic base to abstract the C-4β proton of a steroid substrate, 5-AND (5-androstene-3,17-dione) [17]. One of the interesting features of Asp[38] is that the residue is relatively rigid, even though it is exposed to solvent and is located near the flexible loop between β-strands B1 and B2 (Figure 1). The KSI monomer from *C. testosteroni* has five proline residues, the isomerization of which is known to affect the folding process of KSI [20]. Only Pro[39] has a *cis*-configuration [12], which can confer structural strain on Asp[38]. Pro[39] is conserved in the two KSIs, and is so closely located to Asp[38] as to give a structural rigidity to the local active-site geometry consisting of Asp[38], Pro[39], Val[40], Gly[41] and Ser[42] due to its cyclic side chain [9,10].

Proline residues are unique among natural amino acids, since the cyclic side chain of proline prevents the rotation of an N–Cα bond, and the peptide backbone has no amide hydrogen for

Abbreviations used: 5-AND, 5-androstene-3,17-dione; ANS, 1-anilinonaphthalene-8-sulphonic acid; *B* factor, average temperature factor; *d*-equilenin, *d*-1,3,5(10),6,8-estrapentaen-3-ol-17-one; ΔG_U^{H2O}, free-energy change for unfolding in the absence of urea at 25.00 $\pm$ 0.02 °C; KSI, ketosteroid isomerase; SH, Src homology; T_m, melting temperature.

[1] To whom correspondence should be addressed (e-mail kchoi@postech.ac.kr).

The atomic coordinates for the crystal structure of P39A in complex with *d*-equilenin have been deposited at Brookhaven Protein Data Bank (code, 1OGZ).

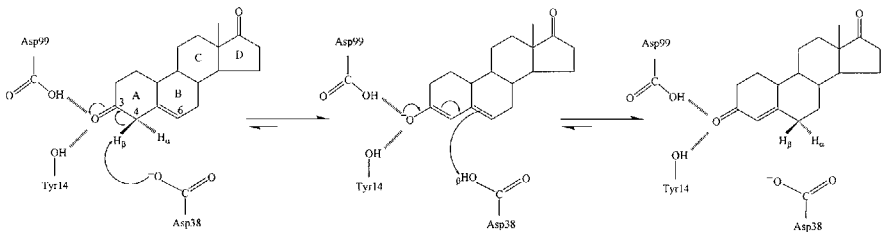

Scheme 1 Mechanism of the KSI-catalysed isomerization of 5-AND

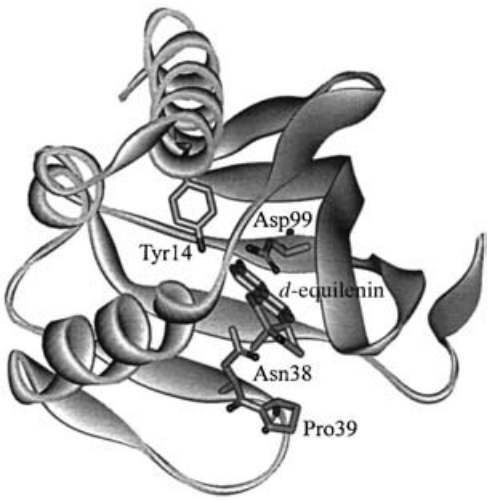

Figure 1 Ribbon diagram of the three-dimensional structure of *C. testosteroni* KSI in complex with *d*-equilenin

Tyr[14], Asn[38], Pro[39], Asp[99] and *d*-equilenin, a reaction intermediate analogue, are shown in a ball and stick model. The KSI structure was generated by the Molscript program [19].

hydrogen bonding. The *trans* isomer is favoured only slightly over the *cis* isomer, since the *cis* and *trans* configurations were reported to differ by only 2.1 kJ/mol (0.5 kcal/mol) in free energy [21–23]. The residue has been reported frequently to be important for the biological function and structural stability of proteins. In case of interleukin-2 tyrosine kinase, *cis*/*trans* isomerization of Pro[287] within the SH2 (Src homology 2) domain acts as a molecular switch that mediates conformer-specific ligand recognition [24]. The self-association of interleukin-2 tyrosine kinase via the SH2 and SH3 domains requires *cis*-Pro[287], and the binding of canonical phosphopeptide is mediated by *trans*-Pro[287] [24,25]. In addition, the *cis*/*trans* isomerization of Pro[175] plays a critical role in electron transport by the membrane protein cytochrome bc_1 [26]. Furthermore, replacement of the proline residue with other amino acids has unfavourable effects on protein stability. For example, the replacement of *cis*-Pro[39] with alanine in RNase T1 substantially reduced ΔG_U^{H2O} (the free-energy change for unfolding in the absence of urea at 25.00 $\pm$ 0.02 °C) by approx. 20.1 kJ/mol (4.8 kcal/mol) [27]. In the case of RNase A, mutation of *cis*-Pro[93] or *cis*-Pro[114] to glycine decreased T_m (the melting temperature) by 7.3 °C and 10.2 °C respectively [28].

In the present study, in order to investigate the structural role of Pro[39] in the catalytic activity and the active-site geometry of *C. testosteroni* KSI, Pro[39] was replaced with alanine or glycine. Both k_{cat} and ΔG_U^{H2O} values were significantly decreased by the P39A and P39G mutations. The crystal structure of the P39A mutant in complex with *d*-equilenin [*d*-1,3,5(10),6,8-estrapentaen-3-ol-17-one], a reaction intermediate analogue, showed structural perturbations of Asp[38] and the local active site near Asp[38], which resulted in substantial decreases in the catalytic activity and conformational stability of KSI. Our results demonstrate that the conserved *cis*-Pro[39] residue is important for both the proper positioning of the critical catalytic residue Asp[38] and the structural integrity of the active site in KSI.

MATERIALS AND METHODS

Reagents

Ultrapure urea was purchased from Sigma. T4 DNA ligase and restriction enzymes were obtained from Roche Molecular Biochemicals. ANS (1-anilinonaphthalene-8-sulphonic acid) was purchased from Molecular Probes. Oligonucleotides were obtained from Bionics Inc. 5-AND was purchased from Steraloid Inc. 5-AND exhibited a single spot on TLC analysis and its molecular mass was confirmed by MS, as described previously [29]. All other chemicals were molecular biology grade and obtained from Sigma.

Site-directed mutagenesis

The conserved *cis*-Pro[39] residue was replaced with alanine or glycine to make the P39A and P39G mutants respectively, using a method described previously [30]. Single-stranded and uracil-containing template DNA complementary to the coding strand of the KSI gene was obtained from pKSI-TI [9], a recombinant plasmid containing the entire gene of *C. testosteroni* KSI, which had been introduced into *Escherichia coli* RZ1030 after infection with the helper phage M13K07 (Amersham Pharmacia Biotech). The oligonucleotides 5′-GCCACGGTGGAAGACCG-CCGTGGGTTCCGAGC-3′ for P39A and 5′-GGCCACGGTG-GAAGACGGCGTGGGTTCCGAGCC-3′ for P39G were used as a primer for each mutagenesis; the underlined nucleotides represent those changed for mutations. The entire genes of the mutant KSIs were sequenced to confirm the presence of the desired mutations. The recombinant plasmid containing the mutated KSI gene was digested with *Eco*RI and *Hin*dIII to isolate the inserted DNA fragment containing the entire KSI gene, which was then subcloned into the *Eco*RI and *Hin*dIII sites of pKK223-3 (Amersham Pharmacia Biotech) to construct the recombinant plasmid for expression. The KSI proteins were expressed in *E. coli* BL21(DE3), and protein concentrations were determined utilizing the difference in molar absorption coefficient (2330 $M^{-1} \cdot cm^{-1}$ per tyrosine residue) between tyrosinate and tyrosine at 295 nm, as described previously [31].

Solvent-accessible surface area

The solvent-accessible surface area was calculated from the atomic co-ordinates obtained by X-ray crystallography [9] utilizing a software program (Molecular Simulations Inc.; Quanta version 2.0) according to the procedures described previously [32]. The probe radius for the calculation was 1.4 Å (1 Å $\equiv$ 0.1 nM).

Determination of catalytic activities and kinetic parameters

The catalytic activities of the wild-type and mutant KSIs were measured spectrophotometrically using 5-AND as a substrate according to the procedure described previously [18]. All enzyme activities were determined by use of a UV spectrophotometer (Cary; 3E) at 25.0 $\pm$ 0.1 °C in a buffer solution containing 34 mM potassium phosphate, pH 7.0, and 2.5 mM EDTA with various substrate concentrations: 12, 35, 58, 82 and 116 μM. The kinetic parameters of the wild-type and mutant KSIs were determined using a non-linear least-squares method, as described previously [33].

pH–activity profiles

All buffers used to determine kinetic constants were adjusted to have constant ionic strength ($I = 0.1$) with NaCl. The buffers were 20 mM sodium acetate (pH 3.8–4.9), 20 mM sodium Mes (pH 5.2–6.3) and 20 mM potassium phosphate (pH 6.6–8.0) at 25.0 $\pm$ 0.1 °C. The reaction procedures for obtaining kinetic constants were the same as for the steady-state kinetic analysis described above. Stability was confirmed by incubating the enzyme in the respective assay buffer for 2 min and then determining enzyme activity at pH 7.0. The observed kinetic parameters were fitted to eqn (1) to obtain the pK_E value by non-linear least-squares analysis using the program Kaleidagraph version 3.06 (Abelbeck Software).

$$(k_{cat}/K_m)_{obs} = (k_{cat}/K_m)/(1 + [H^+]/K_E) \quad (1)$$

Fluorescence spectroscopy

Fluorescence was measured by use of a spectrofluorimeter (Shimadzu; RF-5401) equipped with a thermostatically controlled cell holder. For fluorescence measurements, 15 μM KSI was incubated at 25.0 $\pm$ 0.1 °C in a buffer containing 20 mM potassium phosphate, pH 7.0, and 1 mM EDTA. Emission spectra were observed between 300 and 400 nm after the KSI sample was excited at 275 nm.

CD spectroscopy

CD spectroscopic analyses were performed with a spectropolarimeter (Jasco; 715). A cuvette with a path length of 2 mm was used for all CD spectral measurements. The temperature of the cuvette was adjusted by use of a Peltier-type temperature controller (Jasco; PTC-348WI). For the CD measurements, wild-type or mutant enzyme at 15 μM was incubated in buffer containing 20 mM potassium phosphate, pH 7.0, and 1 mM EDTA. CD spectra were obtained at 25.00 $\pm$ 0.02 °C with a scan speed of 10 nm/min and a bandwidth of 2 nm. Scans were collected at 1 nm intervals, with a response time of 0.25 s, and were accumulated three times. All CD spectra were corrected by subtracting the spectrum of the buffer solution.

Equilibrium unfolding

Wild-type or mutant enzyme at 15 μM was preincubated for > 48 h in buffer containing 20 mM potassium phosphate, pH 7.0, and 1 mM EDTA with various urea concentrations from 0 to 8 M. Molar ellipticity at 222 nm and fluorescence intensity at 304 nm were determined at each urea concentration.

Changes in the optical properties of the KSI proteins were compared by normalizing each transition curve with the apparent fraction of the unfolded form, F_U:

$$F_U = (Y_N - Y)/(Y_N - Y_U) \quad (2)$$

where Y is the observed molar ellipticity or fluorescence intensity at a given urea concentration, and Y_N and Y_U are the observed values for the native and unfolded forms respectively at the same urea concentration. A linear dependence of Y on the denaturant concentration was observed in the baseline regions of both native and unfolded KSIs for both CD and fluorescence spectroscopic measurements. The respective baselines for native and unfolded KSIs were extrapolated linearly to estimate Y_N and Y_U in the transition region.

The equilibrium constant (K_U) and free-energy change (ΔG_U) for denaturation were determined according to a two-state model of denaturation by using the following equations [34]:

$$K_U = 2P_T \cdot \left[{F_U}^2/(1 - F_U)\right] \quad (3)$$

$$\Delta G_U = -RT \cdot \ln(K_U) = {\Delta G_U}^{H2O} - m \cdot [\text{urea}] \quad (4)$$

where P_T is the total protein concentration and m is a measure of the dependence of ΔG_U on urea concentration. The data of the urea unfolding transition curve were fitted to eqn (4) as described previously [35] by a non-linear least-squares analysis utilizing a graphics program (Abelbeck Software; Kaleidagraph version 2.6).

$$Y = Y_N - (Y_N - Y_U) \cdot \exp\left[\left(m \cdot [\text{urea}] - {\Delta G_U}^{H2O}\right)/RT\right] \cdot \left(\left\{1 + 8P_T/\exp\left[\left(m \cdot [\text{urea}] - {\Delta G_U}^{H2O}\right)/RT\right]\right\}^{1/2} - 1\right)/4P_T \quad (5)$$

The difference in the free-energy change for unfolding, $\Delta\Delta G_U$, between the wild-type enzyme and each mutant enzyme was obtained from the following equation:

$$\Delta\Delta G_U = \Delta G_U - {\Delta G_U}^m \quad (6)$$

where ΔG_U and ${\Delta G_U}^m$ are the free-energy changes for unfolding of the wild-type and mutant KSIs respectively.

Crystallization and structure determination of the P39A KSI mutant in complex with *d*-equilenin

The P39A mutant was co-crystallized with *d*-equilenin by the hanging-drop vapour-diffusion method according to the procedure described previously [10]. A 2 μl aliquot of 1 mg/ml equilenin dissolved in DMSO was mixed with 70 μl of 10 mg/ml KSI. Saturation with equilenin was comfirmed by the presence of a white precipitate formed after mixing. The crystals were grown in a solution containing 2.0 M ammonium sulphate and 0.1 M Tris/HCl, pH 8.5, at 22.0 $\pm$ 0.1 °C. For data collection, the crystal was frozen at 100 K utilizing a cryostream cooler (Oxford Cryosystems) after it was briefly immersed in a cryoprotectant solution containing 15 % (v/v) glycerol, 2.0 M ammonium sulphate

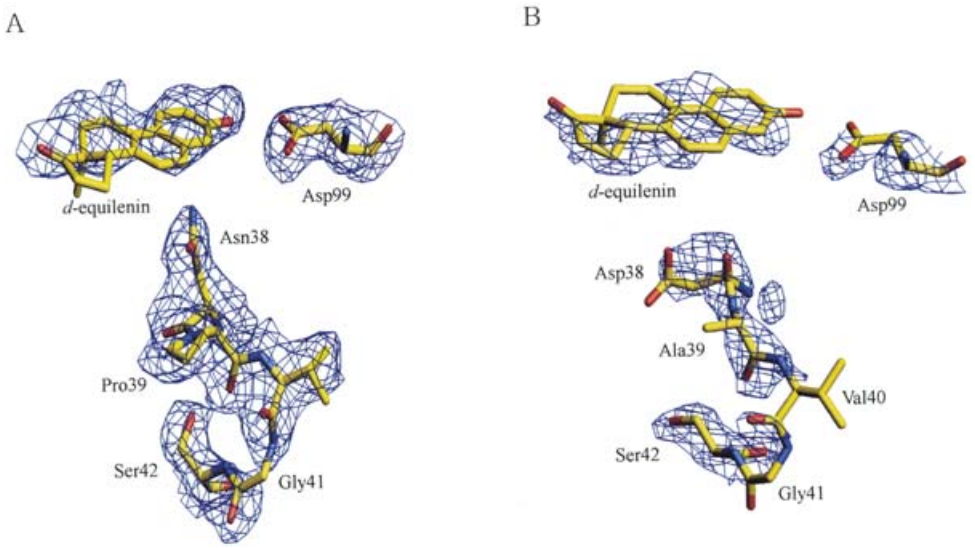

Figure 2 $2F_o$–F_c electron density maps of the local structure surrounding residue 39 near the active site of KSI for D38N–equilenin (A) and P39A–equilenin (B)

The crystal structures of D38N–equilenin and P39A–equilenin were displayed utilizing graphic software *O* [19]. The electron density contoured at 1.0 σ was calculated with the final refined structure. The original backbones and side chains in the crystal structure of D38N–equilenin are traced as heavy lines to compare with those of P39A–equilenin, where the electron densities of Ala[39], Val[40], Gly[41] and *d*-equilenin are poorly defined.

and 0.1 M Tris/HCl, pH 8.5. Diffraction data were obtained by use of synchrotron radiation from beamline 6B at Pohang Light Source, Pohang, Korea. Data reduction, merging and scaling were carried out with the programs DENZO and SCALEPACK, as described previously [36]. The crystal structure of P39A KSI in complex with *d*-equilenin (P39A–equilenin) was determined by molecular replacement utilizing the dimeric structure of wild-type KSI [9] as a search model according to the method described previously [10].

Determination of K_d for equilenin

The dissociation constant (K_d) for equilenin was determined by the fluorescence quenching method as described previously [37]. Fluorescence measurement was carried out at 25.0 $\pm$ 0.1 °C with a spectrofluorimeter (Shimazu RF-5000) in a buffer solution containing 10 mM potassium phosphate, pH 7.0, and 5 % (v/v) methanol. The fluorescence intensity of equilenin at 363 nm was obtained and used to calculate K_d values for *d*-equilenin after excitation at 335 nm for various enzyme concentrations.

ANS-binding assay

Binding experiments with ANS were performed by incubating the wild-type and mutant proteins with ANS. KSI (15 μM) was incubated with 25 μM ANS at 25.0 $\pm$ 0.1 °C in a buffer solution containing 20 mM potassium phosphate, pH 7.0, and 1 mM EDTA. Fluorescence changes were monitored between 400 and 600 nm after the incubated solution was excited at 380 nm. Fluorescence spectra were obtained by a fluorescence spectrophotometer (Shimadzu RF-5401) using a cuvette with a path length of 10 mm, and the spectrum of the ANS solution without enzyme was subtracted.

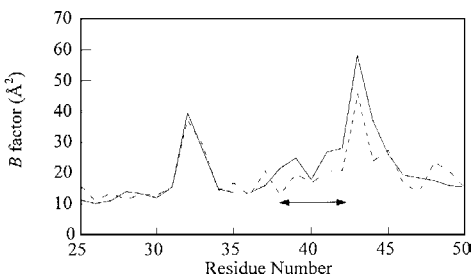

Figure 3 *B* factors for the main-chain atoms in *C. testosteroni* KSI with (broken line) and without (solid line) *d*-equilenin

The arrow indicates Asp[38], Pro[39], Val[40], Gly[41] and Ser[42] located at the loop between β-strands B1 and B2. *B* factors of the Cα atoms in the crystal structure of D38N–equilenin [10] were used for comparison with those of KSI alone [9].

RESULTS

Structural aspects of the conserved *cis*-Pro[39] residue near the active site of KSI

Based on three-dimensional structural analysis of wild-type KSI, the side chain of Pro[39] is structurally associated with Asp[38] (Figure 1) [9,10]. The side chain of Asp[38] interacts with *d*-equilenin at the active-site pocket. The pyrrolidine ring in the side chain of Pro[39] is covalently linked to the polypeptide backbone of the preceding Asp[38] residue. Val[40], Gly[41] and Ser[42] near Pro[39] constitute a loop spanning β-strands B1 and B2 (Figure 2), and their solvent-accessible surface areas are 14, 22, and 6 Å^2 respectively, indicating that they are well or partially exposed to the aqueous environment. While Asp[38], with a solvent-accessible surface area of 16 Å^2, is exposed to solvent and located near the flexible loop between β-strands B1 and B2, its *B* factor (average temperature factor) was found to be relatively small, and much smaller again when *d*-equilenin was bound to the enzyme (Figure 3).

Table 1 Kinetic parameters for the isomerization of 5-AND catalysed by wild-type and mutant KSIs

The assays were performed in a buffer containing 34 mM potassium phosphate and 2.5 mM EDTA, pH 7.0, at 25.0 ± 0.1 °C. The kinetic parameters were obtained from three independent measurements. Relative values are compared with the wild-type enzyme.

Enzyme	k_{cat} (s^{-1})	K_m (μM)	k_{cat}/K_m ($M^{-1} \cdot s^{-1}$)	Relative k_{cat}	Relative K_m
Wild type	32 000 ± 1200	150 ± 6	$(2.10 \pm 0.07) \times 10^8$	1.0	1.0
P39A	475 ± 12	42 ± 1	$(1.20 \pm 0.03) \times 10^7$	1.5×10^{-2}	0.3
P39G	33 ± 1	31 ± 1	$(1.10 \pm 0.03) \times 10^6$	1.1×10^{-3}	0.2

Expression and purification of KSI proteins

Both mutant proteins P39A and P39G were expressed as inclusion bodies. The inclusion bodies were dissolved with 8 M urea and then dialysed with a refolding buffer containing 20 mM potassium phosphate, pH 7.0, and 1 mM EDTA. The mutant proteins were purified similarly to the wild-type enzyme [9]. The homogeneity of the purified mutant proteins was confirmed by the presence of single protein bands of an identical size corresponding to a monomer molecular mass of approx. 14 kDa upon SDS/PAGE (results not shown).

Effects of mutation of Pro[39] on the catalytic activity of KSI

In order to analyse the effects of the P39A and P39G mutations on the catalytic activity of KSI, the k_{cat} and K_m values of the wild-type and mutant KSIs were determined using 5-AND as a substrate. Elimination of the pyrrolidine ring from Pro[39] resulted in more significant effect on k_{cat} than on K_m. The P39A and P39G mutations decreased the K_m values moderately (by approx. 3.6- and 4.8-fold respectively) and the k_{cat} values significantly (by approx. 67- and 970-fold respectively) compared with the wild-type enzyme (Table 1). These results suggest that the cyclic side chain of Pro[39] is important for the catalytic activity of KSI.

pH–activity profiles

In a previous study, the catalytic base Asp[38] was proposed to be responsible for the pH-dependent activity of KSI [4]. In order to estimate the pK_a value of Asp[38] in the wild-type and mutant enzymes, the kinetic parameters of the wild-type and mutant proteins were determined at various pH values (Figure 4). The observed kinetic parameters were fitted to eqn (1) to obtain the apparent pK_E value. The pK_E value of wild-type KSI was determined to be approx. 4.32 [37a], which was comparable with that in the previous study [4]. The apparent pK_E values of P39A and P39G were 4.36 and 4.31 respectively, indicating that Pro[39] does not affect the ionization state of Asp[38].

Effects of mutation of Pro[39] on the conformational stability of KSI

An equilibrium unfolding experiment was carried out by measuring the molar ellipticity of the P39A and P39G mutants at 222 nm and the fluorescence intensity at 304 nm after excitation at 275 nm. The transition curve was normalized by assuming that the optical properties of the native and unfolded KSIs can be extrapolated linearly into the transition zone (Figure 5). The transition curves obtained by measuring molecular ellipticity and fluorescence intensity were almost identical to each other. These results strongly suggest that the folding of KSI can be explained by

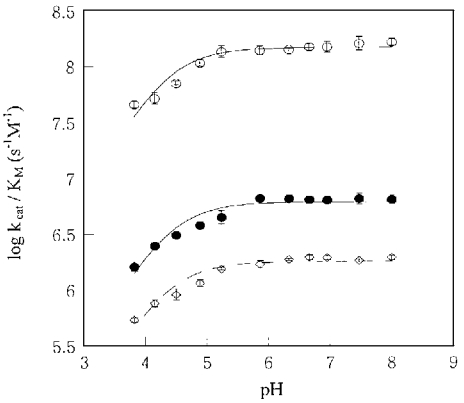

Figure 4 pH-dependence of kinetic parameters of wild-type and mutant KSIs

The kinetic parameters of the wild-type and mutant enzymes were determined at various pH values at 25.0 ± 0.1 °C. The lines represent non-linear least-squares fits of the data to eqn (1) in order to obtain pK_E. 5-AND was used as a substrate, and log k_{cat}/K_m values are shown for the wild type (○), P39A (●) and P39G (◇) enzymes.

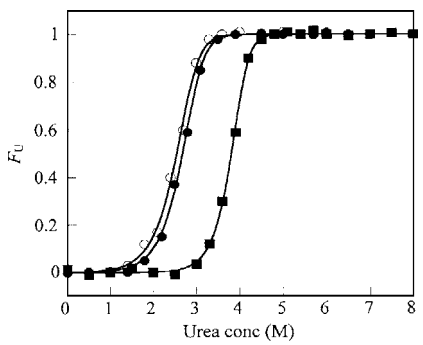

Figure 5 Unfolding equilibrium transition curves of wild-type, P39A and P39G KSIs

The fraction of unfolded protein (F_U) at each urea concentration was calculated from the molar ellipticity at 222 nm and the fluorescence intensity at 304 nm with excitation at 275 nm after correction for the pre- and post-transition baselines and fitting to eqn (5). F_U values for the wild type (■), P39A (●) and P39G (○) enzymes are shown.

a two-state model, without any folded intermediate at equilibrium. The reversible folding of the KSI mutants was analysed by comparing fluorescence and CD spectra of the protein being refolded with those of the native protein. The unfolded protein in 8 M urea was diluted successively to lower urea concentrations under reducing conditions. All mutants also exhibited the original activities after refolding. Based upon the two-state model, the values of ΔG_U^{H2O}, m, $[\text{urea}]_{50\%}$ and $\Delta\Delta G_U$ for the wild-type and mutant KSIs were determined (Table 2). The P39A and P39G mutations significantly decreased ΔG_U^{H2O} by approx. 31.0 and 35.6 kJ/mol (7.4 and 8.5 kcal/mol) respectively, suggesting that Pro[39] is important for the conformational stability of KSI. The effect of the P39G mutation on protein stability was more pronounced than that of P39A. The unfolding transitions of both P39A and P39G mutants occurred at lower urea concentrations than that of the wild-type enzyme. In the transition curves of the P39A and P39G mutants, significant changes in optical properties were not observed until the urea concentration reached 1.5 M. A drastic transition was observed in the range 1.5–3.5 M urea.

Table 2 Free-energy changes of equilibrium unfolding of wild-type and mutant KSIs

The equilibrium unfolding experiment was carried out by measuring the molar ellipticity of the enzymes at 222 nm and the fluorescence intensity at 304 nm after excitation at 275 nm at pH 7.0. Values were obtained by fitting the data from Figure 5 to eqn (5). ΔG_U^{H2O} was determined by extrapolation of the data to a urea concentration at 0 M during denaturation. m is the slope of the linear denaturation plot, $d\Delta G_U/d[urea]$. $[Urea]_{50\,\%}$ is the urea concentration at which 50 % of the protein is unfolded. $\Delta\Delta G_U$ values were obtained from eqn (6). Note 1 kcal = 4.184 kJ.

Enzyme	ΔG_U^{H2O} (kcal/mol)	m (kcal/mol · M)	$[Urea]_{50\,\%}$ (M)	$\Delta\Delta G_U$ (kcal/mol)
Wild type	22.0 ± 0.5	4.00 ± 0.07	4.25 ± 0.10	–
P39A	14.6 ± 0.7	2.82 ± 0.11	2.78 ± 0.16	7.4
P39G	13.5 ± 0.4	2.76 ± 0.06	2.55 ± 0.09	8.5

Table 3 Crystallographic data and refinement statistics for the crystal structure of P39A mutant KSI in complex with *d*-equilenin

R_{sym}, $[|I_{obs} - I_{avg}|]/I_{obs}$, where I_{obs} is an individual intensity measurement, and I_{avg} is the average intensity for this reflection summed over all the data; $R_{standard}$, $[|F_o| - |F_c|]/|F_o|$, where $|F_o|$ and $|F_c|$ are the observed and calculated structure factor amplitudes respectively; R_{free}, R factor for a test set of unique reflections that have been omitted from the refinement process; rmsd, root-mean-square deviation.

Parameter	Value
Resolution (Å)	2.3
R_{sym} (%)	6.5
Data completeness, $F > 1\sigma$ (%)	95.3
$R_{standard}$ (%)	23.9
R_{free} (%)	32.0
Number of atoms	1097
Water molecules	133
Average *B* factor	29.99
rmsd bond length deviation (Å)	0.083
rmsd bond angle deviation (°)	3.172
Ramachandran plot (%)	
Most favoured regions	81.9
Additional allowed regions	16.7
Disallowed regions	1

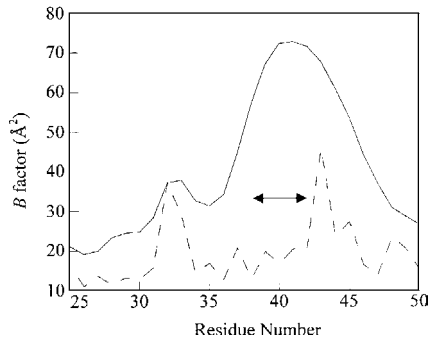

Figure 6 *B* factors for the main-chain atoms in the crystal structures of D38N–equilenin (broken line) and P39A–equilenin (solid line)

The arrow indicates Asn[38] in D38N–equilenin/Asp[38] in P39A–equilenin, and Pro[39], Val[40], Gly[41] and Ser[42] located at the loop between β-strands B1 and B2. *B* factors of the Cα atoms in the crystal structure of D38N–equilenin [10] were used for comparison with those of P39A–equilenin.

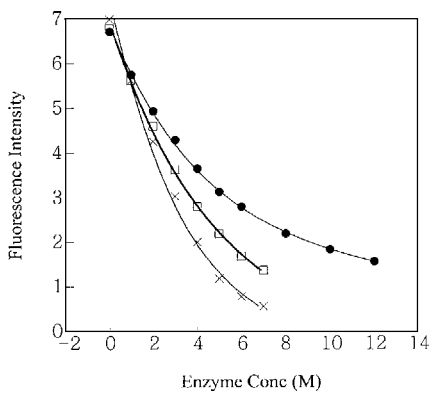

Figure 7 Fluorescence quenching at 363 nm of *d*-equilenin bound to wild-type (●), P39A (□) and P39G (×) KSI

Structural analysis of the P39A–equilenin complex

In order to investigate the structural changes induced by the P39A and P39G mutations at the molecular level, we attempted to crystallize the mutant enzymes with or without various steroids, and crystals of P39A in complex with equilenin were obtained successfully. The crystal structure of P39A–equilenin was determined at 2.3 Å resolution with an *R* value of 23.9 %. It belongs to the space group *P*6522 with cell dimensions of: *a*, 60.73 Å; *b*, 60.73 Å; *c*, 180.80 Å; γ, 120.00. The crystallographic data and refinement statistics are summarized in Table 3. Since no crystallographic data are available for the wild-type enzyme in complex with *d*-equilenin, the crystal structure of P39A–equilenin was compared with that of a D38N mutant KSI in complex with *d*-equilenin (D38N–equilenin), which gives us structural information on the binding interaction between KSI and the steroid in the catalytic reaction of KSI [7,10]. Even though the overall protein structure was not changed significantly, as judged by the structural comparison between D38N–equilenin and P39A–equilenin, the local structure around Pro[39] and the structural geometry of Asp[38] were perturbed by eliminating the five-membered pyrrolidine ring of the proline. The carboxy group in the side chain of Asp[38] was oriented away from β-face of *d*-equilenin (Figure 2), and the distance between Oδ-1 in the side chain of Asp[38] and C-4 of *d*-equilenin was greatly increased by 3.40 ± 0.32 Å. The *B* factor for the Cα atom of Asp[38] was increased significantly by 44 Å^2 (Figure 6). Moreover, the electron-density maps of *d*-equilenin, Ala[39], Val[40] and Gly[41] were poorly defined (Figure 2), and the *B* factors of Ala[39], Val[40], Gly[41] and Ser[42] at the loop between β-strands B1 and B2 were increased substantially in the crystal structure of P39A–equilenin (Figure 6).

Effects of mutation of Pro[39] on binding of equilenin to KSI

The P39A mutant was found to disrupt the proper orientations of both Asp[38] and *d*-equilenin in the structural analysis of P39A–equilenin. In order to investigate the effects of mutations on the binding affinity for *d*-equilenin, the K_d values of the wild-type, P39A and P39G enzymes were determined by measuring the extent of quenching of the fluorescence of *d*-equilenin upon binding the enzymes (Figure 7). The K_d value of the wild-type enzyme was determined to be approx. 2.60 μM, which was similar to that in a previous study [7]. The P39A and P39G mutations decreased the K_d value only by approx.1.9- and 2.3-fold respectively relative to wild-type KSI (Table 4), indicating that they did not change significantly the binding affinity for the reaction intermediate analogue.

Table 4 Dissociation constants of *d*-equilenin for wild-type and mutant KSIs

K_d values for *d*-equilenin were determined by measuring the fluorescence change of equilenin upon protein binding, as described previously [37]. The experiments were carried out in buffer containing 10 mM potassium phosphate and 5 % (v/v) methanol, pH 7.2, at 25.0 ± 0.1 °C. Values are means ± S.D.from three independent measurements.

Enzyme	K_d (μM)
Wild type	2.6 ± 0.1
P39A	1.4 ± 0.1
P39G	1.1 ± 0.1

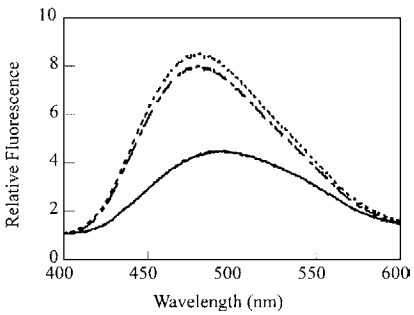

Figure 8 Fluorescence spectra of ANS with wild-type (solid line), P39A (dashed line) and P39G (dotted line) KSI

Excitation was at 380 nm.

Interaction with ANS

To assess the exposed hydrophobic surface areas of the wild-type and mutant enzymes, binding experiments with ANS were carried out. ANS, a fluorescent probe, has been utilized previously in order to monitor conformational changes of the protein, with the subsequent exposure of hydrophobic sites, as described in [38,39]. When the wild-type enzyme was incubated with ANS, the fluorescence intensity was marginally increased (Figure 8). When the P39A and P39G mutants were incubated with ANS, the fluorescence intensities were increased significantly by approx. 2-fold compared with that of the wild-type enzyme with ANS, and the maximum fluorescence wavelengths were blue-shifted from 490 to 478 nm, implying that the mutant KSIs may bind ANS more tightly than does wild-type KSI.

DISCUSSION

The role of the conserved *cis*-Pro[39] residue in the catalytic activity and the conformational stability near the active site of KSI was investigated by replacing this residue with alanine or glycine. Based on the structural analysis of P39A–equilenin and the ANS fluorescence spectra of P39A and P39G, the conserved *cis*-Pro[39] residue was found to be crucial for the proper positioning of the critical catalytic base Asp[38] and for the structural integrity of the active site in KSI. The elimination of the cyclic side chain of Pro[39] disrupted the proper orientation of both Asp[38] and *d*-equilenin, leading to significant decreases in the catalytic activity and the conformational stability of KSI.

The P39A and P39G mutations significantly lowered the k_{cat} value of KSI, even though Pro[39] is not directly involved in binding of the steroid (Figure 1). This result was mainly due to the structural perturbation of Asp[38], which is structurally associated with Pro[39] at the active site of KSI. The P39A and P39G mutations may decrease the rigidity of N–Cα rotation at this position and perturb the configuration of Asp[38], while it did not affect the ionization state of the catalytically important base. Even though the electron density of Asp[38] was defined in the crystal structure of P39A–equilenin, Asp[38] became much more flexible and oriented away from the β-face of *d*-equilenin. In addition, the electron-density map of *d*-equilenin was not well defined in the crystal structure of P39A–equilenin, reflecting the fact that *d*-equilenin is bound less productively to the P39A enzyme than to the wild-type enzyme. These observations strongly suggest that Pro[39] plays an important role in the catalytic activity of KSI through the proper positioning of Asp[38] to abstract stereospecifically the C-4β proton from the substrate steroid.

The substantial decreases in the ΔG_U^{H2O} values of the P39A and P39G mutants compared with the wild type suggest that *cis*-Pro[39] is important for the conformational stability as well as the structural integrity of KSI. Even though Asp[38] is relatively rigid due to the cyclic side chain and the structural strain of the *cis*-Pro[39] residue, it can be structurally perturbed, since it is exposed to solvent and located near the flexible loop between β-strands B1 and B2. The replacement of Pro[39] with a smaller residue, i.e. alanine or glycine, could make the catalytic residue Asp[38] more flexible. Decreases in both the stability and the activity of KSI were observed in the P39A and P39G mutants, implying that stabilization of the local active-site structure near Asp[38] is related to the activity of KSI. While the overall structure was not changed significantly by the P39A and P39G mutations, as reflected in the far-UV CD spectra (results not shown), the crystal structure of P39A–equilenin exhibited significant structural perturbation of the local active-site geometry consisting of Asp[38], Ala[39], Val[40], Gly[41] and Ser[42] at the flexible loop. These observations suggest that the *cis*-Pro[39] residue is crucial for the stabilization of local active-site geometry as well as for the proper positioning of Asp[38] in the active site of KSI. The crystallographic data were found to be consistent with the ANS fluorescence spectra for the P39A and P39G mutants. The perturbed active site near Asp[38] was highly flexible and well exposed to solvent by the P39A mutation; this indicates that ANS may bind better to the P39A and P39G mutants, enhancing ANS fluorescence intensity and blue-shifting the maximum wavelengths of the mutants. The structural significance of the conserved *cis*-Pro[39] residue might also explain the previous observation that the prolyl isomerization accelerated by cyclophilin A, a peptidyl-prolyl isomerase, may be important for the refolding process of KSI [20].

Approx. 6 % of Xaa–Pro peptide bonds in known protein structures have been reported to have *cis* configuration [22,40]. The kinetic barrier for rotation of a Xaa–Pro peptide bond is low enough to allow equilibration of the isomers in an unfolded protein, but high enough to limit the rate of protein folding. The occurrence of *cis*-proline residues in a protein structure often has a significant influence on protein activity and stability [41–45]. In the tryptophan synthase α subunit, the P207A mutant has a less negative CD intensity than the wild-type protein, indicating a role for Pro[207] in maintaining the intact structure [41]. In staphylococcal nuclease, a P31A mutation led to a small decrease in stability of 2.5 kJ/mol (0.6 kcal/mol), and P117G and P117T mutations affected the folding process [42]. In the case of pancreatic RNase A, mutation of conserved two *cis*-proline residues (P93A, P39S, P114A and P114S) has been shown to induce decreases in stability of 8.4–12.6 kJ/mol (2–3 kcal/mol) [43]. For bovine adrenodoxin, mutation of the conserved Pro[108] residue (P108A, P108S, P108W and P108K)

decreased stability by 5.0–10.7 kJ/mol [44]. The mutational effect was more substantial for *E. coli* thioredoxin, where a P76A mutation decreased T_m from 82 to 65 °C [45], indicating that proline is important for protein stability. Proline is also known to be important for catalytic activity through the maintenance of active-site integrity in some proteins. In *E. coli* aspartate transcarbamoylase, the conserved *cis*-Pro^{268} residue is located near the preceding Leu^{267} residue, whose carbonyl oxygen interacts with the nitrogen of the bisubstrate analogue *N*-phosphonacetyl-L-aspartate bound at the active site [46–48]. Replacement of *cis*-Pro^{268} with alanine resulted in a 40-fold decrease in activity, and altered the tertiary structure of the catalytic subunit [49]. In functional analysis of the conserved *cis*-Pro^{53} residue in *Proteus mirabilis* glutathione transferase B1-1, *cis*-Pro^{53} was found to contribute to activity through the maintenance of the proper conformation of the binding site for glutathione [50]. Thus the above examples emphasize the importance of *cis*-Pro residues for the conformational stability and structural integrity of the active site in proteins.

In summary, our results demonstrate that the conserved *cis*-Pro^{39} residue plays a crucial role in the proper positioning of the catalytic base Asp^{38} and in maintaning the structural integrity of the local active-site geometry near Asp^{38} in *C. testosteroni* KSI. The significant effects of the P39A and P39G mutations on the k_{cat} value suggested that Pro^{39} is important for catalytic activity even though this residue is not directly involved in the catalytic mechanism of KSI. These studies will contribute to a better understanding of the role of the proline residue in protein structure. Further investigation is required to explore the observation that the *cis*/*trans* isomerization of Pro^{39} is important for the correct folding of KSI.

This research was supported by grants from the program of the National Research Laboratory sponsored by the Korean Ministry of Science and Technology, and from the Korea Science and Engineering Foundation. G. H. N. and B. H. H. were supported in part by the Brain Korea 21 project. Experiments at beamline 6B of Pohang Light Source were supported in part by Korean Ministry of Science and Technology and POSCO.

REFERENCES

1 Ha, N. C., Choi, G., Choi, K. Y. and Oh, B.-H. (2001) Structure and enzymology of Delta5-3-ketosteroid isomerase. Curr. Opin. Struct. Biol. **11**, 674–678
2 Kuliopulos, A., Talalay, P. and Mildvan, A. S. (1990) Combined effects of two mutations of catalytic residues on the ketosteroid isomerase reaction. Biochemistry **29**, 10271–10280
3 Choi, G., Ha, N. C., Kim, S. W., Kim, D.-H., Park, S., Oh, B.-H. and Choi, K. Y. (2000) Asp-99 donates a hydrogen bond not to Tyr-14 but to the steroid directly in the catalytic mechanism of Δ^5-3-ketosteroid isomerase from *Pseudomonas putida* biotype B. Biochemistry **39**, 903–909
4 Pollack, R. M., Bantia, S., Bounds, P. L. and Koffman, B. M. (1986) pH dependence of the kinetic parameters for 3-oxo-Δ^5-steroid isomerase. Substrate catalysis and inhibition by (3S)-spiro[5α-androstane-3,2-oxiran]-17-one. Biochemistry **25**, 1905–1911
5 Xue, L., Kuliopulos, A., Mildvan, A. S. and Talalay, P. (1991) Catalytic mechanism of an active-site mutant (D38N) of Δ^5-3-ketosteroid Isomerase: Direct spectroscopic evidence for dienol intermediates. Biochemistry **30**, 4991–4997
6 Hawkinson, D. C., Eames, T. C. and Pollack, R. M. (1991) Energetics of 3-oxo-Δ^5-steroid isomerase: source of the catalytic power of the enzyme. Biochemistry **30**, 10849–10858
7 Hawkinson, D. C., Pollack, R. M. and Ambulos, Jr, N. P. (1994) Evaluation of the internal equilibrium constant for 3-oxo-Δ^5-steroid isomerase using the D38E and D38N mutants: the energetic basis for catalysis. Biochemistry **33**, 12172–12183
8 Kim, S. W., Cha, S.-S., Cho, H.-S., Kim, J.-S., Ha, N.-C., Cho, M.-J., Joo, S., Kim, K.-K., Choi, K. Y. and Oh, B.-H. (1997) High-resolution crystal structures of delta5-3-ketosteroid isomerase with and without a reaction intermediate analogue. Biochemistry **36**, 14030–14036
9 Cho, H.-S., Choi. G., Choi, K. Y. and Oh, B.-H. (1998) Crystal structure and enzyme mechanism of Δ^5-3-ketosteroid isomerase from *Pseudomonas testosteroni*. Biochemistry **37**, 8325–8330
10 Cho, H.-S., Ha, N.-C., Choi, G., Kim, H.-J., Lee, D., Oh, K. S., Kim, K. S., Lee, W., Choi, K. Y. and Oh, B.-H. (1999) Crystal structure of Δ^5-3-ketosteroid isomerase from *Pseudomonas testosteroni* in complex with equilenin settles the correct hydrogen bonding scheme for transition state stabilization. J. Biol. Chem. **274**, 32863–32868
11 Wu, Z. R., Ebrahimian, S., Zawrotny, M. E., Thornbur, L. D., Perez-Alvarado, G. C., Brothers, P., Pollack, R. M. and Summers, M. F. (1997) Solution structure of 3-oxo-Δ^5-steroid isomerase. Science **276**, 415–418
12 Massiah, M. A., Abeygunawardana, C., Gittis, A. G. and Milvan, A. S. (1998) Solution structure of Δ^5-3-ketosteroid isomerase complexed with the steroid 19-nortestosterone hemisuccinate. Biochemistry **37**, 14701–14712
13 Kim, S. W. and Choi, K. Y. (1995) Identification of active site residues by site-directed mutagenesis of Δ^5-3-ketosteroid isomerase from *Pseudomonas putida* biotype B. J. Bacteriol. **177**, 2602–2605
14 Kim, S. W., Joo, S., Choi, G., Cho, H.-S., Oh, B.-H. and Choi, K. Y. (1997) Mutational analysis of the three cysteines and active-site aspartic acid 103 of ketosteroid isomerase from *Pseudomonas putida* biotype B. J. Bacteriol. **179**, 7742–7749
15 Ogez, J. R., Tivol, W. F. and Benisek, W. F. (1977) A novel chemical modification of delta 5-3-ketosteroid isomerase occurring during its 3-oxo-4-estren-17 beta-yl acetate-dependent photoinactivation. J. Biol. Chem. **252**, 6151–6155
16 Benson, A. M., Jarabak, J. and Talalay, P. (1971) The amino acid sequence of Δ^5-3-ketosteroid isomerase of *Pseudomonas testosteroni*. J. Biol. Chem. **246**, 7514–7525
17 Linden, K. G. and Benisek, W. F. (1986) The amino acid sequence of a Δ^5-3-oxosteroid isomerase from *Pseudomonas putida* biotype B. J. Biol. Chem. **261**, 6454–6460
18 Kim, S. W., Kim, C. Y., Benisek, W. F. and Choi, K. Y. (1994) Cloning, nucleotide sequence and overexpression of the gene coding for Δ^5-3-ketosteroid isomerase from *Pseudomonas putida* biotype B. J. Bacteriol. **176**, 6672–6676
19 Kraulis, P. J. (1991) MOLSCRIPT: a program to produce both detailed and schematic plots of protein structures. J. Appl. Crystallogr. **24**, 946–950
20 Kim, D.-H., Jang, D. S., Nam, G. H. and Choi, K. Y. (2001) Folding mechanism of ketosteroid isomerase from *Comamonas testosteroni*. Biochemistry **40**, 5011–5017
21 Stewart, D. E., Sarkar, A. and Schultz, D. A. (1990) Occurrence and role of *cis* peptide bonds in protein structures. J. Mol. Biol. **214**, 253–260
22 MacArthur, M. W. and Thornton, J. M. (1991) Influence of proline residues on protein conformation. J. Mol. Biol. **218**, 397–412
23 Birolo, L., Malashkevich, V. N., Capitani, G., De Luca, F., Moretta, A., Jansonius, J. N. and Marino, G. (1999) Functional and structural analysis of *cis*-proline mutants of *Escherichia coli* partate aminotransferase. Biochemistry **38**, 905–913
24 Mallis, R. J., Brazin, K. N., Fulton, D. B. and Andreotti, A. H. (2002) Structural characterization of a proline-driven conformational switch within the Itk SH2 domain. Nat. Struct. Biol. **9**, 900–905
25 Brazin, K. N., Mallis, R. J., Fulton, D. B. and Andreotti, A. H. (2002) Regulation of the tyrosine kinase Itk by the peptidyl-prolyl isomerase cyclophilin A. Proc. Natl. Acad. Sci. U.S.A. **99**, 1899–1904
26 Iwata, S., Lee, J. W., Okada, K., Lee, J. K., Iwata, M., Rasmussen, B., Link, T. A., Ramaswamy, S. and Jap, B. K. (1998) Complete structure of the 11-subunit bovine mitochondrial cytochrome *bc-1* complex. Science **281**, 64–71
27 Mayr, L. M., Landt, O., Hahn, U. and Schmid, F. X. (1993) Stability and folding kinetics of ribonuclease T1 are strongly altered by the replacement of *cis*-proline 39 with alanine. J. Mol. Biol. **231**, 897–912
28 Schultz, L. W., Hargraves, S. R., Klink, T. A. and Raines, R. T. (1998) Structure and stability of the P93G variant of ribonuclease A. Protein Sci. **7**, 1620–1625
29 Choi, G., Ha, N.-C., Kim, M.-S., Hong, B.-H., Oh, B.-H. and Choi, K. Y. (2001) Pseudoreversion of the catalytic activity of Y14F by the additional substitution(s) of tyrosine with phenylalanine in the hydrogen bond network of Δ^5-3-ketosteroid isomerase from *Pseudomonas putida* biotype B. Biochemistry **40**, 6828–6835
30 Kunkel, T. A., Roberts, J. D. and Zakour, R. A. (1987) Rapid and efficient site-specific mutagenesis without phenotypic selection. Methods Enzymol. **154**, 367–382
31 Copeland, R. A. (1993) Methods of Protein Analysis, Chapman and Hall, New York
32 Conolly, M. L. (1983) Analytical molecular surface calculation. Science **221**, 709–713
33 Boyer, P. D. (1970) In The Enzymes. Vol. II: Kinetics and Mechanism, pp. 1–65, Academic Press, New York
34 Kim, D.-H., Jang, D. S., Nam, G. H., Choi, G., Kim, J.-S., Ha, N.-C., Kim, M.-S., Oh, B.-H. and Choi, K. Y. (2000) Contribution of the hydrogen-bond network involving a tyrosine triad in the active site to the structure and function of a highly proficient ketosteroid isomerase from *Pseudomonas putida* biotype B. Biochemistry **39**, 4581–4589
35 Mok, Y.-K., Gay, G. D., Butler, P. J. and Bycroft, M. (1996) Equilibrium dissociation and unfolding of the dimeric human papillomavirus strain-16 E2 DNA-binding domain. Protein Sci. **5**, 310–319

36 Otwinowski, Z. (1993) In Proceedings of the CCP4 Study Weekend: Data Collection and Processing (Sawyer, L., Issacs, N. and Bailey, S., eds.), pp. 56–62, SERC Daresbury Laboratory, Warrington, U. K.
37 Kim, D. H., Nam, G. H., Jang, D. S., Choi, G., Joo, S., Kim, J. S., Oh, B. H. and Choi, K. Y. (1999) Roles of active site aromatic residues in catalysis by ketosteroid isomerase from *Pseudomonas putida* biotype B. Biochemistry **38**, 13810–13819
37a Yun, Y. S., Lee, T.-H., Nam, G. H., Jang, D. S., Shin, S., Oh, B.-H. and Choi, K. Y. (2003) Origin of the different pH activity profile in two homologous ketosteroid isomerases. J. Biol. Chem. **287**, 28229–28236
38 Johnson, J. D., El-Bayoumi, M. A., Weber, L. D. and Tulinsky, A. (1979) Interaction of alpha-chymotrypsin with the fluorescent probe 1-anilinonaphthalene-8-sulfonate in solution. Biochemistry **18**, 1292–1296
39 Nam, G. H. and Choi, K. Y. (2002) Association of human tumor necrosis factor-related apoptosis inducing ligand with membrane upon acidification. Eur. J. Biochem. **269**, 5280–5287
40 Maigret, B., Perhia, D. and Pullman, B. (1970) Molecular orbital calculations on the conformation of polypeptides and proteins. IV. The conformation of the prolyl and hydroxyprolyl residues. J. Theor. Biol. **29**, 275–291
41 Yutani, K., Hayashi, S., Sugai, Y. and Ogasahara, K. (1991) Role of conserved proline residues in stabilizing tryptophan synthase alpha subunit: analysis by mutants with alanine or glycine. Proteins Struct. Funct. Genet. **9**, 90–98
42 Nakano, T., Antonino, L. C., Fox, R. O. and Fink, A. L. (1993) Effect of proline mutations on the stability and kinetics of folding of staphylococcal nuclease. Biochemistry **32**, 2534–2541
43 Schultz, D. A. and Baldwin, R. L. (1992) *Cis* proline mutants of ribonuclease A. I. Thermal stability. Protein Sci. **1**, 910–916
44 Grinberg, A. V. and Bernhardt, R. (1998) Effect of replacing a conserved proline residue on the function and stability of bovine adrenodoxin. Protein Eng. **11**, 1057–1064
45 Kelley, R. F. and Richards, F. M. (1987) Replacement of proline-76 with alanine eliminates the slowest kinetic phase in thioredoxin folding. Biochemistry **26**, 6765–6774
46 Krause, K. L., Voltz, K. W. and Lipscomb, W. N. (1987) 2.5 Å structure of aspartate carbamoyltransferase complexed with the bisubstrate analog N-(phosphonacetyl)-L-aspartate. J. Mol. Biol. **193**, 527–553
47 Ke, H.-M., Lipscomb, W. N., Cho, Y. and Honzatko, R. B. (1988) Complex of N-phosphonacetyl-L-aspartate with aspartate carbamoyltransferase. X-ray refinement, analysis of conformational changes and catalytic and allosteric mechanisms. J. Mol. Biol. **204**, 725–747
48 Jin, L., Stec, B., Lipscomb, W. N. and Kantrowitz, E. R. (1999) Insights into the mechanisms of catalysis and heterotropic regulation of Escherichia coli aspartate transcarbamoylase based upon a structure of the enzyme complexed with the bisubstrate analogue N-phosphonacetyl-L-aspartate at 2.1 Å. Proteins Struct. Funct. Genet. **37**, 729–742
49 Jin, L., Stec, B. and Kantrowitz, E. R. (2000) A *cis*-proline to alanine mutant of E. coli aspartate transcarbamoylase: kinetic studies and three-dimensional crystal structures. Biochemistry **39**, 8058–8066
50 Allocati, N., Casalone, E., Masulli, M., Ceccarelli, I., Carletti, E., Parker, M. W. and Di Ilio, C. (1999) Functional analysis of the evolutionarily conserved proline 53 residue in *Proteus mirabilis* glutathione transferase B1-1. FEBS Lett. **445**, 347–350

Received 17 February 2003/27 June 2003; accepted 10 July 2003
Published as BJ Immediate Publication 10 July 2003, DOI 10.1042/BJ20030263